Natural Hazards (2024) 120:12851–12867
https://doi.org/10.1007/s11069-024-06721-y

ORIGINAL PAPER

Exploring building vibration dynamics in the wake of the Chi-Chi earthquake: implications for natural hazard preparedness

David Ching-Fang Shih[1] · **Yih-Min Wu**[2]

Received: 17 October 2023 / Accepted: 30 May 2024 / Published online: 7 June 2024
© The Author(s), under exclusive licence to Springer Nature B.V. 2024

Abstract
This study delves into the critical realm of natural hazard preparedness by examining building vibrations after Taiwan's Chi-Chi earthquake (1999). By meticulously analyzing the monitored displacement of a building pre- and post-catastrophe, we unveil a notable correlation between the building's proximity to the hypocenter and subsequent changes in period and damping as earthquake magnitudes escalate. Based on these insights, we have devised a robust regression model to accurately estimate optimal periods using peak ground acceleration values. Our research provides a pragmatic assessment of a building's innate vibration characteristics, crucial for long-term seismic monitoring, with a focus on an attic-basement system. The findings offer a fresh perspective on how buildings respond to catastrophic earthquakes, shedding light on their resilience. Moreover, this study demonstrates the feasibility and practicality of evaluating a building's vibration evolution through comprehensive historical strong motion data. Our work provides valuable insights for future maintenance and safety considerations, ensuring steadfast structural integrity in the face of natural hazards.

Keywords Building vibration · Earthquake safety assessment · Dynamic behaviour · Chi-Chi earthquake · Natural hazard

1 Introduction

Taiwan, situated along the western Circum-Pacific seismic belt, experiences significant tectonic activity. The convergence of the Philippine Sea plate beneath the Eurasian plate at the Ryukyu trench and the eastward subduction of the South China Sea lithosphere under the Philippine Sea plate contribute to intense crustal deformation and faulting

✉ David Ching-Fang Shih
dcfshih@gmail.com; cfshih@nari.org.tw

Yih-Min Wu
drymwu@ntu.edu.tw

[1] National Atomic Research Institute, Longtan, Taoyuan, Taiwan, ROC

[2] Department of Geosciences, National Taiwan University, Taipei, Taiwan, ROC

along this active convergent margin (Shin et al. 2002). With a rapidly developing economy and a proliferation of high-rise buildings, densely populated Taiwan faces escalating risks from seismic hazards.

Satake and Yokota (1996) conducted vibration tests and earthquake observations to analyze the vibration properties of high-rise steel buildings. They found that the natural periods estimated from earthquake records were more extended than those obtained from ambient vibration measurements. Scruggs et al. (2006) proposed a method to minimize the probability of failure in building structures. They used an eight-story base isolation model as a benchmark to demonstrate this approach. Todorovska and Trifunac (2008) emphasized that monitoring only changes in the soil-structure system frequency could be misleading for structural health monitoring. Instead, they suggested tracking fixed-base frequency changes over a specific period as a more reliable approach. Ogawa (2014) reviewed three notable damage cases during the 1995 Hyogoken-Nanbu earthquake. The study examined these phenomena using a proposed response spectrum with a constant damping factor. It explained the transition of natural periods of buildings and the corresponding increase in period with amplitude. Vidal et al. (2014) estimated the first translational period and damping ratio, investigating the changes in dynamic characteristics of low-to-medium rise buildings in Lorca town, Spain, after a strong earthquake. Siringoringo and Fujino (2015) analyzed an asymmetric L-shaped structure consisting of a seven-story and 14-story building with a vertical opening in the Tokyo Bay area. They utilized strong-motion recordings from a base-isolated building during the Great East Japan (Tohoku) Earthquake on March 11, 2011. The analysis revealed a significant shift in the building's frequency during the mainshock, accompanied by substantial acceleration on the superstructure, reaching peak floor accelerations of nearly 300 cm/sec^2.

In July 1992, the Central Weather Administration of Taiwan (CWA) installed strong-motion array systems in selected constructions such as buildings and bridges. By 2007, a total of 62 monitoring operations were established. The selection of structures for installation was based on three considerations: (1) site conditions, including soft soil, soil, and rock; (2) the natural period of the structure, categorized as short structures with a period less than 0.5 sec, medium-height structures with a period between 0.5 and 1.5 sec, and tall structures with a period longer than 1.5 sec, and (3) non-structural but functional importance, such as schools, hospitals, and communication facilities, where the recorded data would have broad applications. The strong-motion array system in a structure consists of five components: accelerometers, communication cables, signal conditioning unit, real-time data acquisition and processing unit, power supply, and telecommunication unit.

The selection of a single building for this study was intentional, serving as a study to deeply explore the specific dynamics and response mechanisms of a building subjected to significant seismic events, such as the Chi-Chi earthquake. This approach enabled us to conduct a detailed and focused analysis of displacement, period, and damping characteristics, which might be obscured when considering multiple buildings. We acknowledge this approach's limitations in generalizability but believe the insights gained provide valuable groundwork for future research, which could include a broader array of buildings. This research presents a practical and groundbreaking assessment method to evaluate the vibration characteristics of the esteemed hospital building, Station TCH. This approach will provide valuable insights before and after the devastating earthquake in Taiwan in 1999. By addressing safety concerns head-on, this study highlights the criticality of implementing effective maintenance and management strategies for the building.

2 Material and methods

2.1 Background information

Station TCH (station code: HWABA2) is a hospital located at coordinates 23.995° N and 121.592° E in the central-east region of Taiwan (Fig. 1). The building is situated on a 14 m thick formation of muddy gravel. The groundwater level is approximately 3.6 m below the ground surface. The structure of the building consists of reinforced concrete columns, walls, and a basement, with reinforcement, shear reinforcement, and concrete strength values of 4200, 2800, and 280 kg/cm^2, respectively. The collected accelerograph data includes recordings of the notable and devastating Chi-Chi earthquake (also called the 921 earthquake) that occurred at 17:47:12.6 UTC on September 20, 1999, in Chi-Chi, Nantou, Taiwan. The earthquake had a magnitude of 7.3 on the Richter scale (Fig. 1). The assessment conducted in this study focuses on the risk evaluation of TCH based on the differences in the simulated period and damping ratio before and after the 921 earthquake. The quake's epicenter was located at 23.85° N and 120.82° E, approximately 9.2 km southwest of Sun Moon Lake, with a depth of 8 km (Chang et al. 2000, 2007). The earthquake occurred along the Chelungpu Fault in western Taiwan (Fig. 1). The fault stretches along the foothills of the Central Mountains in Nantou and Taichung County. Some sections of land near the fault experienced an uplift of up to 7 m. The earthquake caused extensive damage, including the destruction of bridges and severe transportation disruption for weeks. The total impact included 2,416 deaths (including missing individuals), 11443 severe injuries, 44338 destroyed houses, and 41336 houses severely damaged. The Chi-Chi earthquake event is a significant example of extensive strong-motion studies conducted in Taiwan for emergency response and research purposes in seismology and earthquake engineering. Several notable findings and research papers related to the event can be found in the literature, such as Loh (2000) and Teng et al. (2001).

The destructive 921 earthquake had diverse impacts on structures and buildings, potentially altering their natural vibration characteristics. Fortunately, the TCH station remained unscathed, and its robust motion instruments remained unaffected by the calamity. Nonetheless, prioritizing safety necessitates a proactive investigation into potential risks. This study introduces a conceptual framework that employs a single-degree-of-freedom (SDOF) dynamic system to simulate construction vibrations, explicitly focusing on the dynamics of a base-excited system. Over twelve years, a comprehensive collection of 172 seismograms was gathered from a high-quality strong-motion seismometer, capturing significant earthquakes of varying magnitudes. By scrutinizing the strong motion records obtained at both the basement and the pinnacle of the building, accurate estimates for the construction period and damping were established. Employing seismic accelerographs to simulate the building's vibration characteristics offers a dependable approach for long-term risk assessment, effectively addressing uncertainties associated with its innate response.

2.2 Methodology

Accelerometers are commonly placed in the basement and upper floors or other vital spots as part of a strong-motion array arrangement. The movement recorded in the basement is often seen as indicative of ground shaking. Simultaneously, the motion detected at the building's top encompasses ground shaking and the building's reaction. It's standard

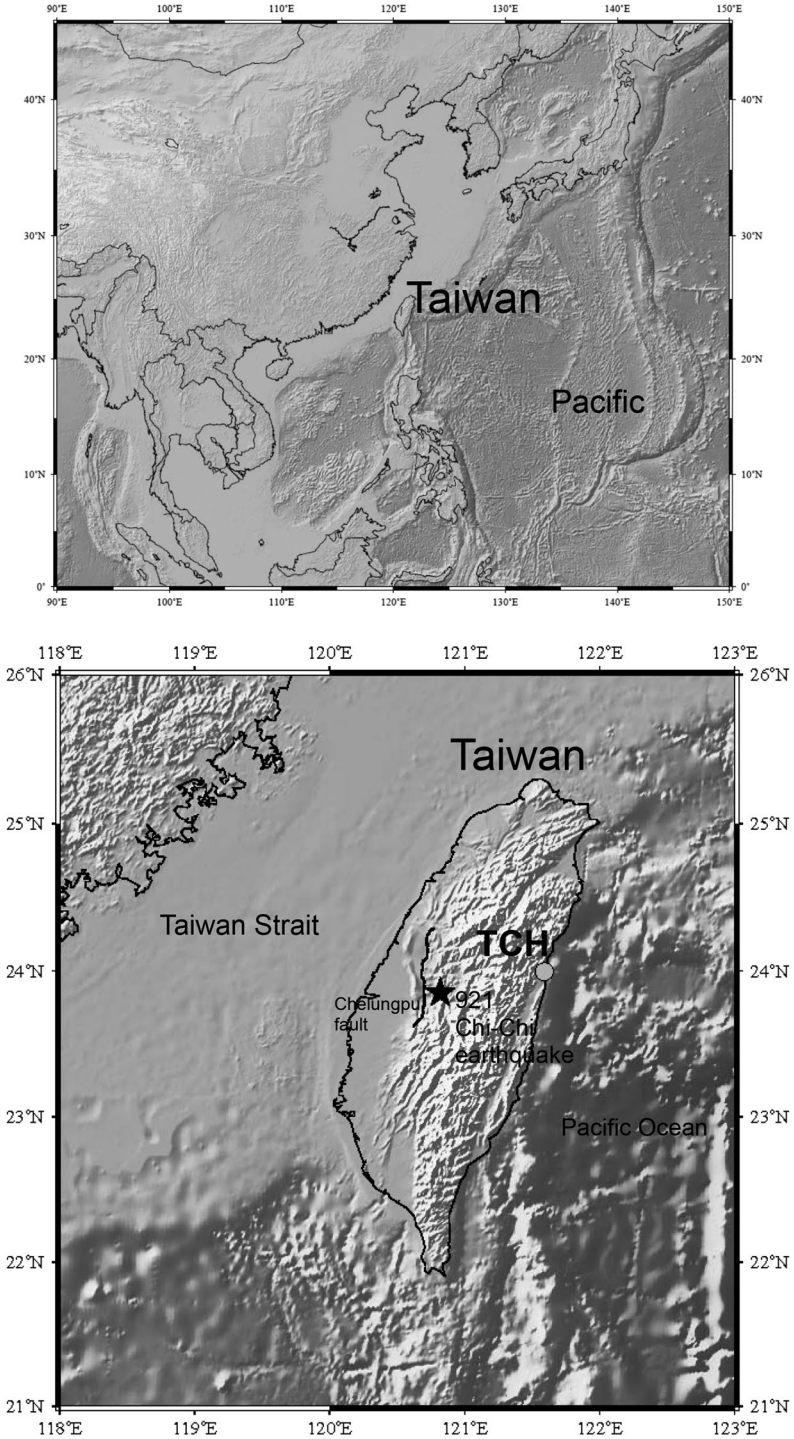

Fig. 1 Maps show the location of the earthquake 921 and studied building TCH

practice to examine data from both locations to distinguish between the effects of ground shaking and the building's behavior. (Amadio et al. 2003; Jangid 2004; Snieder & Safak 2006; Zerva et al. 1996) Traditionally, this process is performed in the frequency domain. However, this study proposes a simplified approach that can be adapted for analysis in the time domain. We chose to use a single degree of freedom (SDOF) model in our study for its simplicity and effectiveness in illustrating basic dynamic principles and facilitating an understanding of the seismic response behaviors of buildings. We acknowledge that this model might not capture all the complexities of high-rise buildings, which would benefit from more complex modeling approaches such as Multiple Degrees of Freedom (MDOF) systems. However, the SDOF model provides a foundation from which more intricate models can be developed and offers valuable insights into the fundamental vibration characteristics of structures. The building is assumed to behave as a single-degree-of-freedom vibration system, and the responses at the basement and top of the building are used to describe its behavior.

$$\frac{d^2x(t)}{dt^2} + 2h\omega_0 \frac{dx(t)}{dt} + \omega_0^2 x(t) = -a(t). \tag{1}$$

where h is the damping ratio (damping),$\omega_0 = 2\pi/T$ (1/sec), T is the natural period (sec), $a(t)$ is the acceleration of basement shaking (cm/sec^2), $d^2x(t)/dt^2$ is the shaking of the top of the building (cm/sec^2). One can regard $a(t)$ as input for the specific system and $d^2x(t)/dt^2$ is the time-dependent output observation by guessing the best value of h and T.

The optimal estimation is obtained by selecting suitable parameters h and T that minimize the squared error between the observed shaking in the attic and the calculated second derivative of displacement for time. This process aims to find values of h and T that best fit between the observed and computed shaking. Kanamori et al. (1999) have proposed a practical approach for this computation. Figures 2 and 3 present a schematic view of the target building from different perspectives, providing visual aids for understanding its structure and orientation.

It performs the optimal estimation by selecting suitable parameters h and T according to that minimum squared error for observed shaking on the attic and calculated $d^2x(t)/dt^2$ can meet; resultant h and T could be the optimal estimation for the building. A helpful process derived by Kanamori et al. (1999) can be performed to achieve the above computation. This research demonstrates a sketch of the target building view in Figs. 2 and 3, which aid in different directions.

The Pearson product-moment correlation coefficient and Spearman rank-order correlation coefficient are employed to assess the correlation between the estimated parameters. The Pearson product-moment correlation coefficient, denoted by r, is a widely used measure of the correlation between two variables. It quantifies the strength and direction of the linear relationship between the variables (Moore 1996). On the other hand, Spearman's rank correlation coefficient, denoted by r_s, is a nonparametric correlation measure. It evaluates how well a monotonic function could describe the relationship between the variables without assuming any specific frequency distribution (Hollander et al. 2013; Kendall 1948; Spearman 1987). These correlation measures provide insights into the relationship between the period and damping of the building's vibration characteristics.

It is important to note that when the correlation coefficients between two variables are positive and the corresponding P-values are below 0.05, they tend to increase together. Conversely, no significant relationship between the variables is observed when the P-values exceed 0.05. The P-value represents the probability of making an

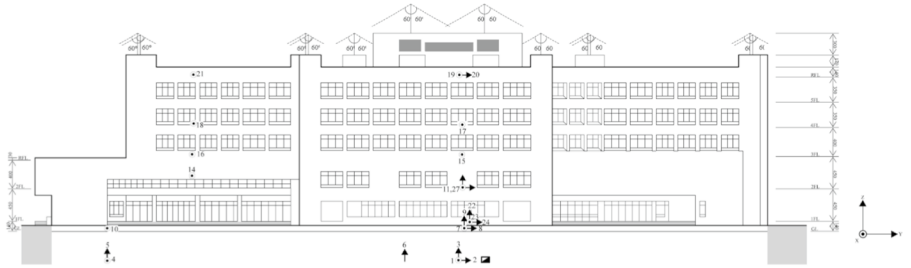

(a) Face to East–South/West–North (E–S/W–N)

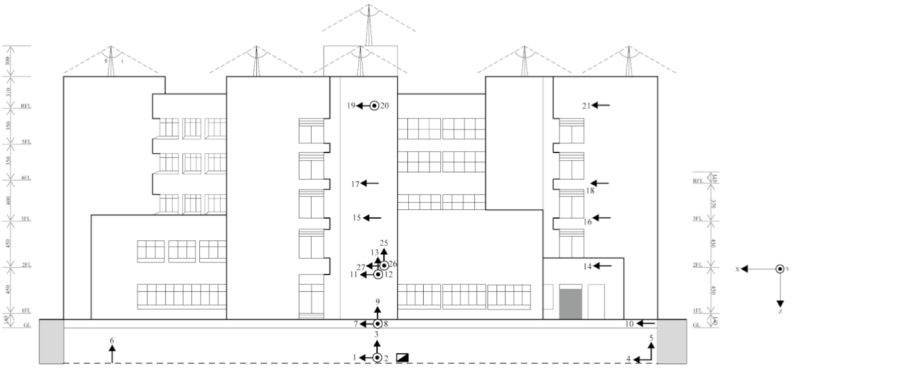

(b) Face to East–North/West–South (E–N/W–S)

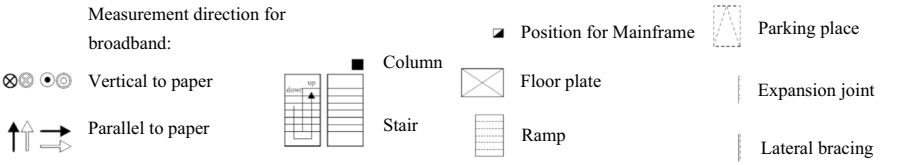

(c) Legend

Fig. 2 Vertical profiles of the building. *Note* numeric in length scale denote cm; scale is in 1/200. The legend of this figure also applies to Fig. 3

incorrect conclusion about the association between the variables, indicating the likelihood of erroneously rejecting the null hypothesis. A smaller *P*-value suggests a higher chance of a correlation between the variables. Traditionally, a *P*-value below 0.05 is considered significant, meaning the independent variable can predict the dependent variable. The Pearson product-moment correlation coefficient and Spearman's rank correlation coefficient methods are suitable for analyzing the correlation between the period and damping in the simulation results, particularly when there is limited background information on the parameters. These methods provide valuable insights into the relationship between these variables and contribute to understanding the system's underlying dynamics.

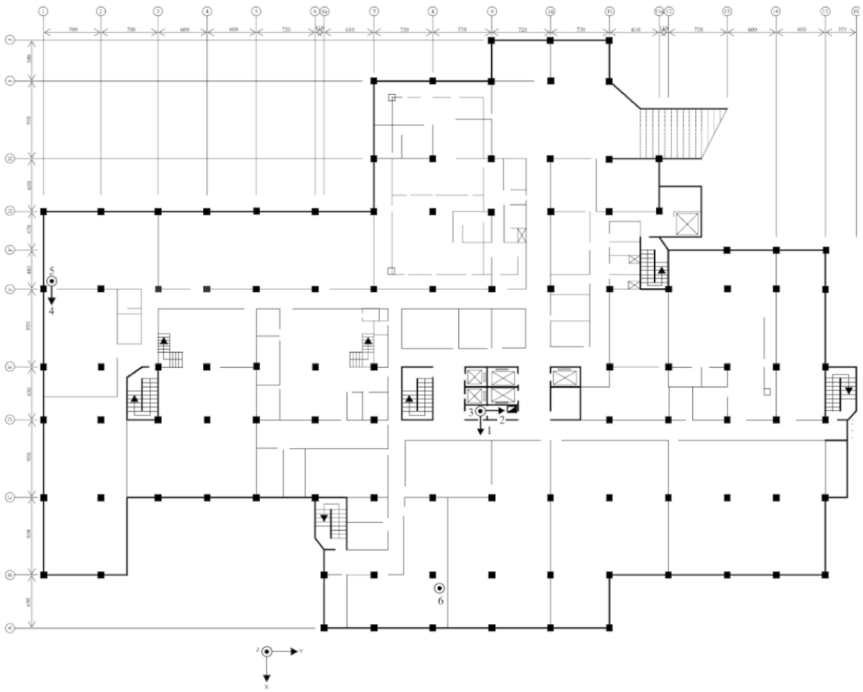

(a) basement

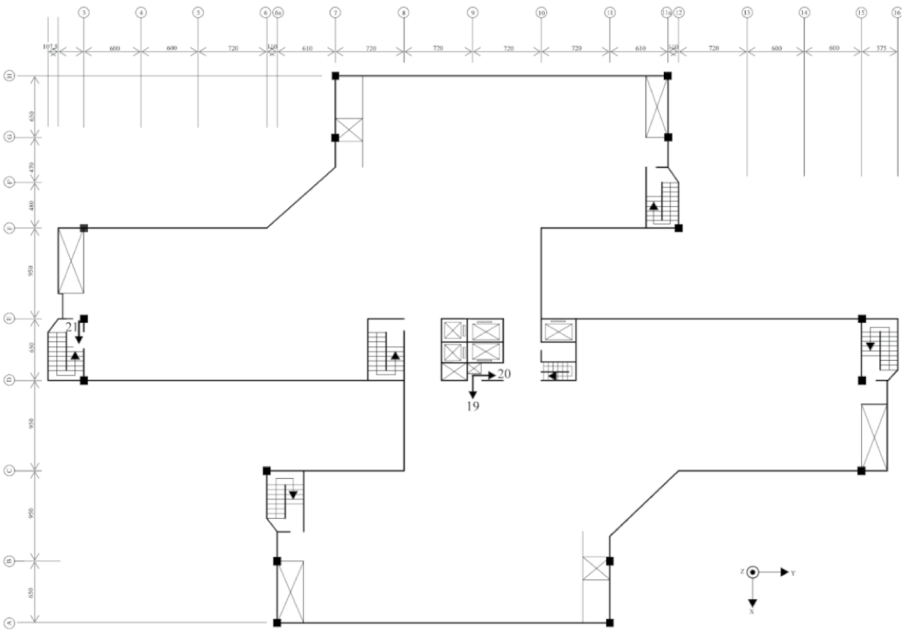

(b) attic

Fig. 3 Top views of the building. *Note* Numeric in length scale denotes cm; scale is in 1/200; the legend of this figure is the same as Fig. 2

2.3 Data

A total of 172 sets of observed accelerographs were collected from 1994, covering approximately 12 years at station TCH. Among these sets, 42 were recorded before the 921 earthquake, while the remaining 130 were recorded after the event. The earthquake magnitudes ranged from 3 to 7.3, with peak ground accelerations ranging from 4 to 156 gal. The distance between the hypocenter and TCH varied from 3 to 229 km. The studied building has two vertical profiles, facing the E–S/W–N and E–N/W–S directions, as depicted in Figs. 2 and 3. For the E–S/W–N direction, input and output responses were obtained from CH1 and CH19 channels in the basement and attic, respectively. Similarly, for the E–N/W–S direction, CH2 and CH20 channels were used for the basement and attic, respectively. It is important to note that CH2 and CH20 are perpendicular to CH1 and CH19, respectively, allowing for a comprehensive analysis of the building's vibration characteristics in different orientations.

To simulate the optimal period and damping values using Eq. (1), the following parameter ranges are selected:

For CH1 and CH19 (CH1 versus CH19):

(1) Period 0.01–0.6 (sec)
(2) Damping 0.005

For CH2 and CH20 (CH2 versus CH20):

(1) Period 0.001–0.06 (sec)
(2) Damping 0.0005

In the simulation, CH1 and CH2 are used as the input records for the forced term a(t), while CH19 and CH20 are the observed response channels for comparing the simulated output obtained from Eq. (1). The sampling rate for all seismograms is set to 200 Hz. The optimal estimation criteria for the period and damping values are determined based on the minimum summation of the squared differences (errors) between the simulated and observed values obtained from CH19 and CH20. By minimizing the error, the simulated results can closely match the observed responses, providing the most accurate estimation for the period and damping of the building's vibration.

3 Results and discussion

The analysis reveals a noticeable trend in the estimated optimal period and damping coefficient for channel CH1 versus CH19 and CH2 versus CH20 (as shown in Figs. 4 and 5) following the 921 earthquake that occurred on September 20, 1999. It is intriguing to observe that, on average, the values for mean, maximum, minimum, median, 25th and 75th percentiles, and standard deviation tend to increase after the 921, except for the range and standard deviation of damping in the case of CH1 versus CH19, which exhibit a decrease (as depicted in Table 1). After the 921 event, there is a decrease in the standard error and confidence interval of the mean for the optimal period and damping. This decrease indicates a higher level of precision in the estimation, as presented in Table 1. The simulated

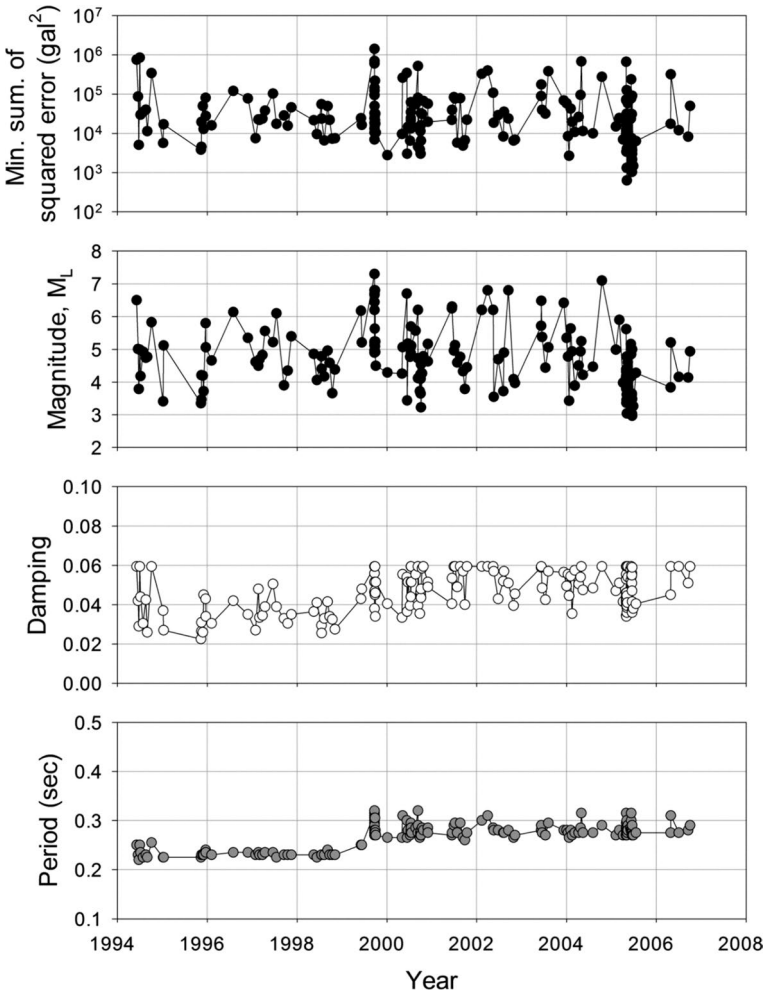

Fig. 4 Estimated optimal period and damping for CH1 versus CH19

responses corresponding to the 921 earthquake for CH1 versus CH19 (Fig. 6) and CH2 versus CH20 (Fig. 7) illustrate the differences between the simulated and observed values. The errors, represented by the differences, are generally within a range of approximately ± 50 gal. These findings provide valuable insights into the changes in period and damping characteristics of the building's vibration following the 921 earthquake, highlighting the impact of seismic events on the structural dynamics.

The analysis using the Pearson product-moment correlation coefficient and Spearman rank-order correlation coefficient reveals a strong correlation, with coefficients exceeding 0.67 and remarkably low *P*-values, for CH1 versus CH19 before and after the 921 earthquake (as indicated in Table 2). It suggests that the period and damping coefficients tend to increase as the responses at the top of the structure reflect the input from the basement. On the other hand, there is no significant relationship between CH2 versus CH20, as evidenced by their low correlation coefficient and higher *P*-value (Table 2). It is worth noting

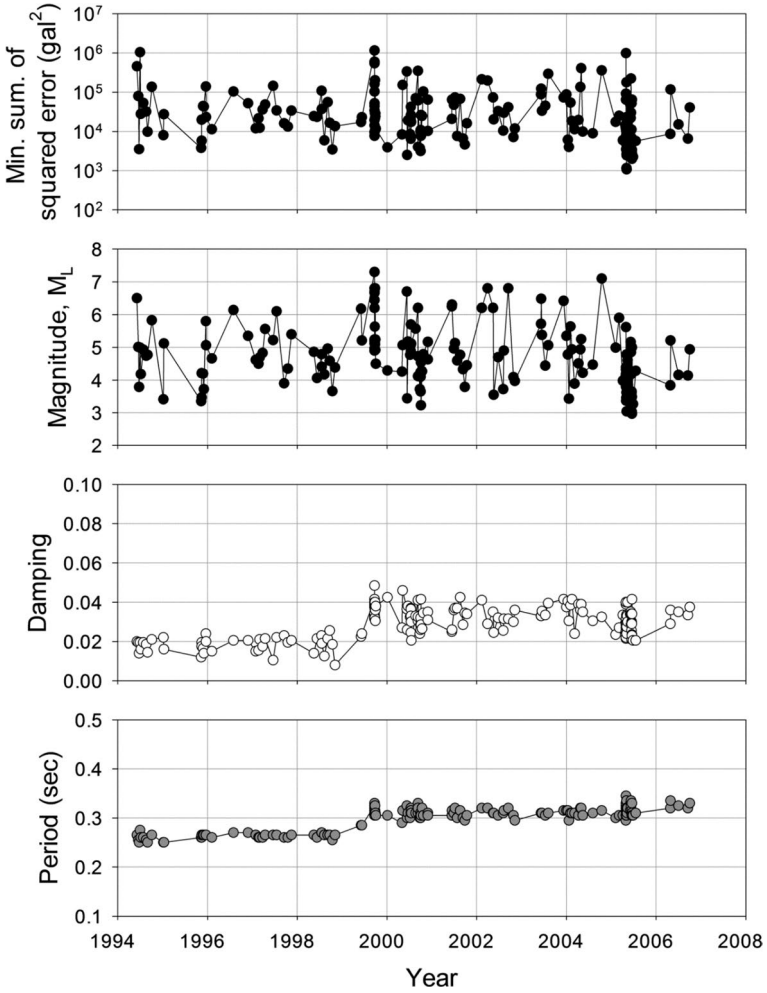

Fig. 5 Estimated optimal period and damping for CH2 versus CH20

that the vibration in the attic, caused by the earthquake's impact on the building's basement, consistently increases the period and damping coefficient for CH1 versus CH19. Figure 8 provides a visual representation of the distribution of period and damping concerning the earthquake's magnitude and the distance between the hypocenter and the receiver. It reveals that, for smaller distances (e.g., less than 50 km), the period and damping tend to increase as the magnitude of the earthquake increases. However, for higher magnitudes (e.g., M_L greater than 6), the period decreases as the distance between the hypocenter and receiver increases. These observations highlight the complex interplay between seismic events, distance, and the resulting period and damping characteristics, shedding light on the dynamic behavior of the building under different earthquake scenarios.

In addition to the analysis above, regression models were employed to examine the relationship between peak ground acceleration (PGA) and the period and damping coefficients following the catastrophic 921 earthquake. It is important to note that the dataset used

Table 1 Descriptive statistics of the best period and damping

	CH1 versus CH19				CH2 versus CH20			
	Before 921		After 921		Before 921		After 921	
	Period (sec)	Damping	Period (sec)	Damping	Period (sec)	Damping	Period (sec)	Damping
Size	42	42	130	130	42	42	130	130
Mean	0.233	0.0370	0.282	0.0500	0.263	0.0185	0.313	0.0325
Range	0.035	0.0370	0.060	0.0260	0.035	0.0175	0.055	0.0280
Maximum	0.255	0.0595	0.320	0.0595	0.285	0.0255	0.345	0.0485
Minimum	0.220	0.0225	0.260	0.0335	0.250	0.0080	0.290	0.0205
Median	0.230	0.0348	0.280	0.0512	0.265	0.0195	0.310	0.0330
25%	0.230	0.0305	0.275	0.0430	0.260	0.0155	0.305	0.0285
75%	0.235	0.0425	0.290	0.0595	0.265	0.0215	0.320	0.0370
Standard deviation	0.00790	0.00939	0.01330	0.00822	0.00756	0.00393	0.00952	0.00588
Standard error	0.00122	0.00145	0.00117	0.00072	0.00117	0.00061	0.00084	0.00052
Confidence interval of mean	0.00246	0.00293	0.00231	0.00143	0.00235	0.00122	0.00165	0.00102

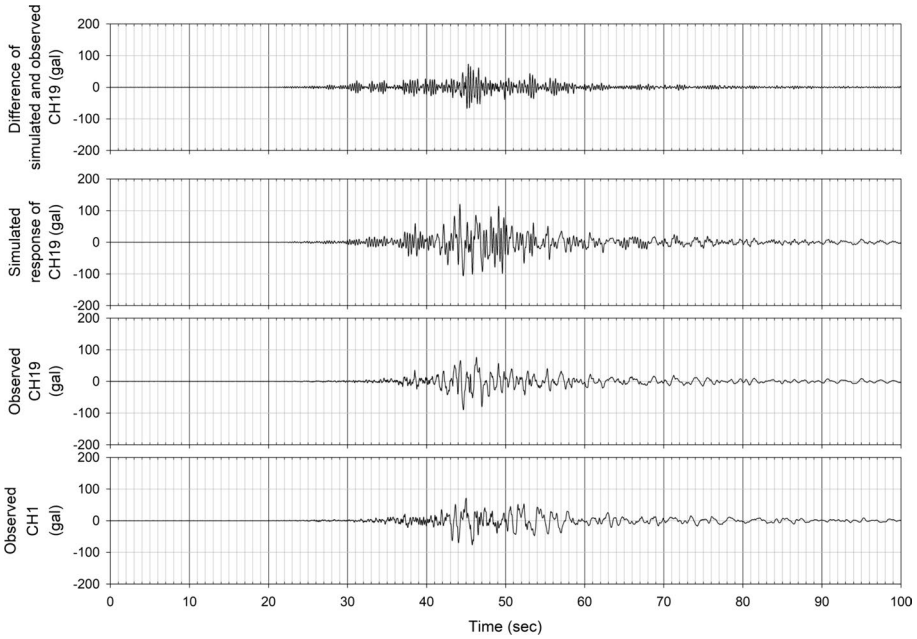

Fig. 6 Simulated and observed response for CH1 versus CH19 for the 921

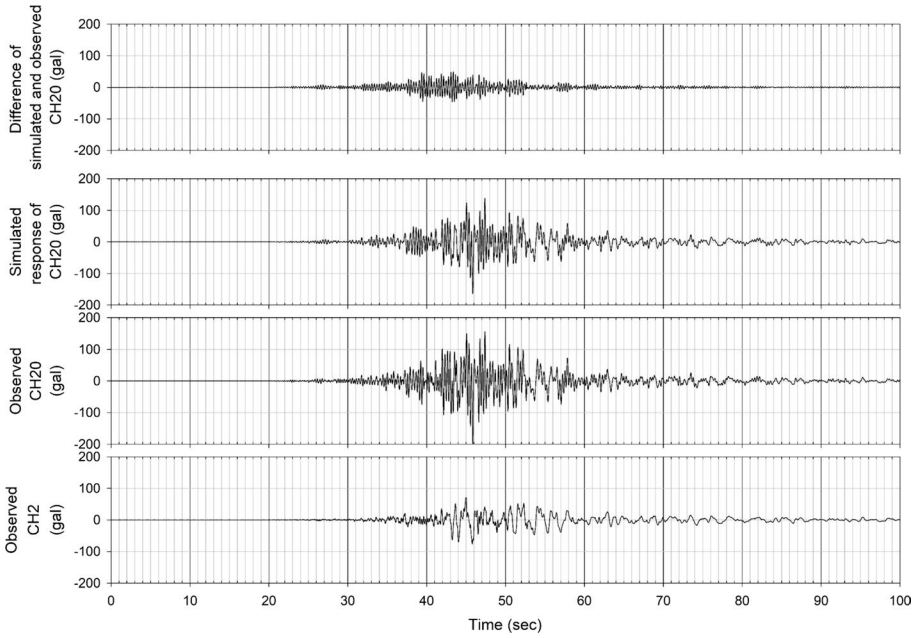

Fig. 7 Simulated and observed response for CH2 versus CH20 for the 921

Table 2 Comparison of the correlations for period and damping estimations

	Channel 1 versus 19		Channel 2 versus 20	
	Before	After	Before	After
Pearson product-moment correlations, r				
Correlation coefficient for period versus damping	0.767	0.677	0.298	0.279
P-value	3.08×10^{-9}	9.76×10^{-19}	5.49×10^{-2}	1.31×10^{-3}
Spearman rank order correlations, r_s				
Correlation coefficient for period versus damping	0.672	0.742	0.302	0.276
P-value	0	0	5.19×10^{-2}	1.53×10^{-3}

"Before" and "after" denote the sample collected before and after the 921

for this analysis does not include data from the 921 event. By excluding the 921 data, the regression analysis focuses on the post-event period and damping characteristics, allowing for a more specific examination of their influence on peak ground acceleration. This analysis provides valuable insights into the relationship between seismic parameters and the resulting ground motion. It offers a deeper understanding of the building's response to earthquakes and its potential vulnerability in subsequent events. It shows:

$$T_e = y_0 + a\left(1 - b^{PGA}\right). \tag{2}$$

where T_e is estimated as the best period, y_0, a, and b are regressed constants presented as 0.2691, 0.0548, and 0.9719, respectively (Fig. 9).

The fascinating analysis unveiled a power relationship between the estimated optimal period and PGA. This intriguing finding suggests a distinct pattern: as PGA increases, the period of vibration tends to follow a specific trend, potentially indicating how the structure responds to varying levels of ground shaking. On the other hand, the damping coefficient did not exhibit a clear relationship that a specific regression model can accurately capture. It implies that PGA may not strongly influence damping or that other influential factors are at play. Further investigation is warranted to unravel the underlying dynamics and mechanisms governing damping with seismic events. These observations emphasize the intricate interplay between seismic parameters and structural response, underscoring the necessity for comprehensive and nuanced approaches in seismic analysis and design. Moreover, the research demonstrates that the majority of the estimated optimal periods fall within the 95% prediction range of the regression model. It suggests that the regression model offers a reliable estimation for the periods of vibration, serving as a valuable tool for predicting the dynamic response of the building.

The analysis also reveals that the estimated optimal damping values remain below 50 gal for the corresponding PGA levels. It indicates that the building's damping characteristics remain relatively stable, suggesting that significant changes in damping behavior are not observed in the aftermath of the 921 earthquake. These findings imply that the targeted building's period and damping properties underwent minimal alterations following the devastating earthquake. As a result, there is no immediate need to make adjustments to the installed sensors in response to the earthquake event.

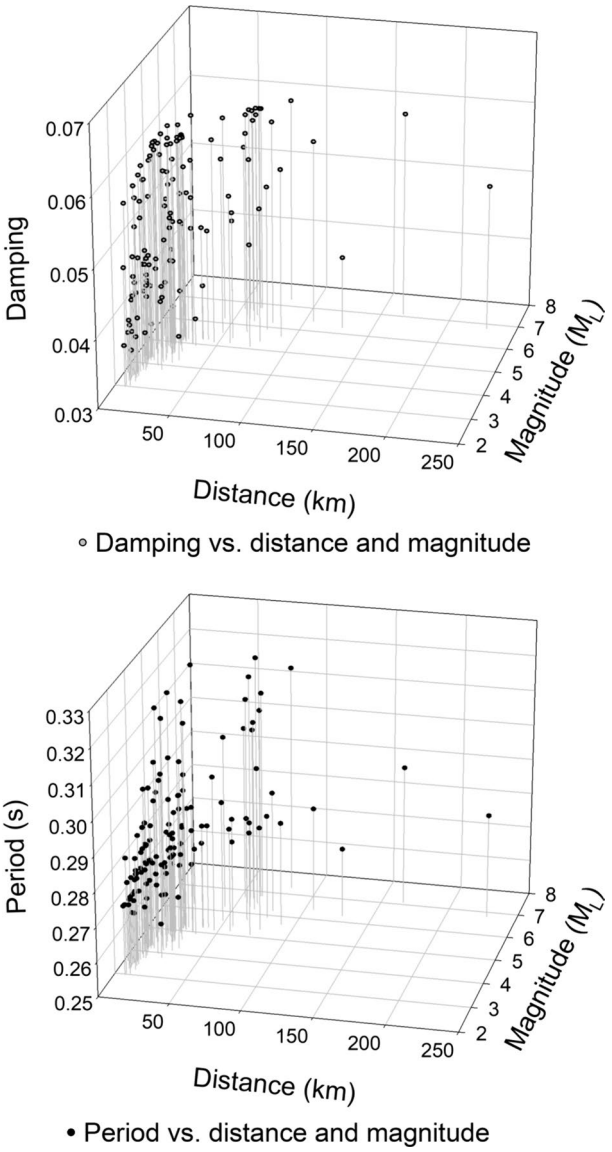

Fig. 8 Estimated optimal period and damping versus earthquake magnitude and distance between hypocenter and targeted building for CH1 versus CH19 after the 921

This research demonstrates the feasibility and practicality of utilizing historical long-term strong motion data to investigate building vibrations and assess the structural condition following a catastrophic earthquake. It emphasizes the potential benefits of leveraging such data to monitor and evaluate the integrity of buildings, particularly in high-risk seismic zones. By employing this approach, practical post-earthquake assessment can be conducted, ensuring the safety and resilience of vital infrastructure. While the current study focuses on a single building, the methodologies employed, such as regression analysis and seismic data to evaluate dynamic responses, apply to other buildings. The regression model developed, for example, is based on principles of structural dynamics that are not unique

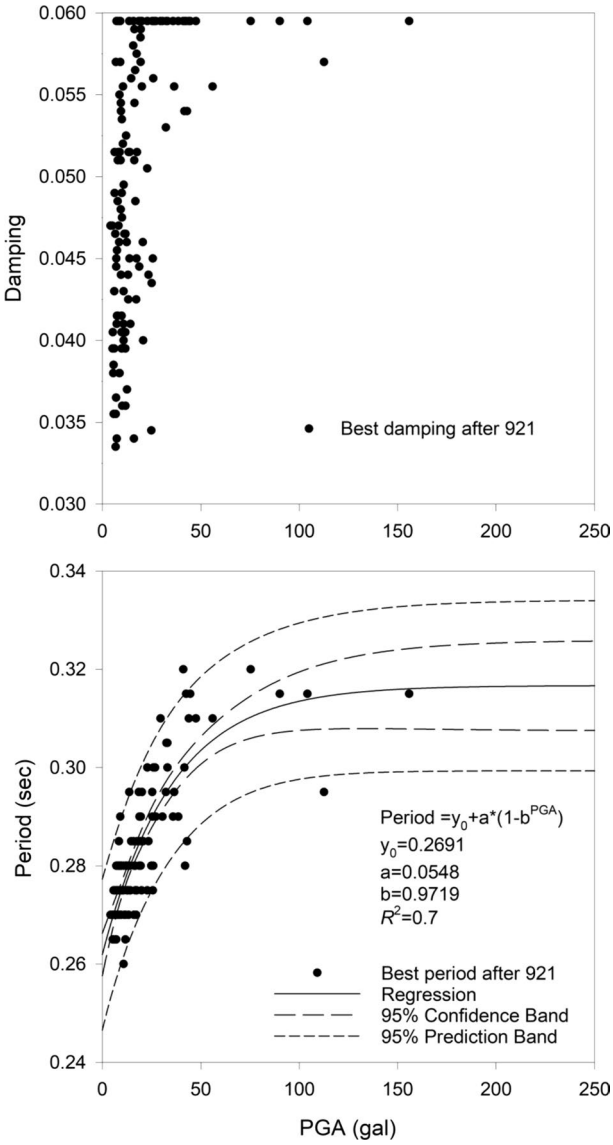

Fig. 9 Regression of period and damping to PGA for CH1 versus CH19, after the 921

to the specific building studied. We suggest future studies could adapt and apply the same analytical framework to other structures to validate and possibly refine our findings.

4 Conclusion

This study centered on analyzing simulated shaking characteristics of a building using a single-degree-of-freedom dynamic system approach. The impact of the Chi-Chi earthquake on the building's vibration characteristics was assessed by examining input and output

responses at basement and attic levels. The earthquake event was a unique opportunity to study essential parameters such as period and damping, crucial for understanding a building's response to seismic activity.

The study found that the targeted building's period and damping experienced slight changes after the 921 earthquake. Correlation analysis revealed an increase in period and damping when input shake from the basement reached the building's top. Additionally, periods and damping increased for earthquake magnitudes less than 50 km from the hypocenter. Conversely, periods decreased for higher magnitudes (above 6) and greater distances.

The study indicated a power function relationship between the estimated optimal period and PGA. Post-earthquake, estimated optimal period and damping exhibited minimal changes. This study showcases a practical approach to assessing a building's natural vibration, allowing for long-term earthquake activity observation. By utilizing historical strong motion data, monitoring a building's status and ensuring its safety becomes feasible. These insights are pivotal for seismic risk management and structural assessment practices, offering a foundation for effective strategies in the face of natural hazards.

Acknowledgements The authors thank the data from the Central Weather Administration of Taiwan to complete this research.

Author contributions David Ching-Fang Shih: Conceptualization, research formulation, methodology, data manipulation and calculation, analysis, manuscription writing, review, and editing. Yih-Min Wu: Data source, calculation tool, and technical support.

Funding This research received no external funding.

Declarations

Conflict of interest The authors declare that no known competing financial interests or personal relationships could influence the work for reporting this paper.

References

Amadio C, Fragiacomo M, Rajgelj S (2003) The effects of repeated earthquake ground motions on the non-linear response of SDOF systems. Earthquake Eng Struct Dynam 32(2):291–308

Chang C-H, Wu Y-M, Shin T-C, Wang C-Y (2000) Relocation of the 1999 Chi-Chi earthquake in Taiwan. Terr Atmos Ocean Sci 11(3):581–590

Chang C-H, Wu Y-M, Zhao L, Wu FT (2007) Aftershocks of the 1999 Chi-Chi, Taiwan, earthquake: the first hour. Bull Seismol Soc Am 97(4):1245–1258

Hollander M, Wolfe DA, Chicken E (2013) Nonparametric statistical methods. John Wiley & Sons, New Jersey

Jangid R (2004) Response of SDOF system to non-stationary earthquake excitation. Earthq Eng Struct Dynam 33(15):1417–1428

Kanamori H, Maechling P, Hauksson E (1999) Continuous monitoring of ground-motion parameters. Bull Seismol Soc Am 89(1):311–316

Kendall MG (1948) Rank correlation methods. Griffin, New York

Loh C-H (2000). Proceedings of international workshop on annual commemoration of Chi-Chi earthquake. National Center for Research on Earthquake Engineering

Moore LM (1996) The basic practice of statistics. Technometrics 38(4):404–405. https://doi.org/10.1080/00401706.1996.10484558

Ogawa Y (2014) Review of damage to buildings during 1995 hyogoken-nanbu earthquake by elasto-plastic response spectrum with constant damping factor. J Struct Constr Eng (Trans AIJ) 79(700):711–720. https://doi.org/10.3130/aijs.79.711

Satake N, Yokota H (1996) Evaluation of vibration properties of high-rise steel buildings using data of vibration tests and earthquake observations. J Wind Eng Ind Aerodyn 59(2–3):265–282

Scruggs J, Taflanidis A, Beck J (2006) Reliability-based control optimization for active base isolation systems. Struct Control Health Monit: Off J Int Assoc Struct Control Monit Eur Assoc Control Struct 13(2–3):705–723

Shin TC, Tsai YB, Yeh YT, Liu CC, Wu YM (2002) Instrumentation programs in Taiwan. In: Lee WH, Jennings P, Kisslinger C, Kanamori H (eds) Strong-motion, international handbook of earthquake and engineering seismology. International Association Seismology and Physics of Earth's Interior, Committee on Education

Siringoringo DM, Fujino Y (2015) Seismic response analyses of an asymmetric base-isolated building during the 2011 Great East Japan (Tohoku) earthquake. Struct Control Health Monit 22(1):71–90

Snieder R, Safak E (2006) Extracting the building response using seismic interferometry: theory and application to the Millikan Library in Pasadena, California. Bull Seismol Soc Am 96(2):586–598

Spearman C (1987) The proof and measurement of association between two things. Am J Psychol 100(3/4):441–471

Teng T-L, Tsai Y-B, Lee WH (2001) Preface to the 1999 Chi-Chi, Taiwan, earthquake dedicated issue. Bull Seismol Soc Am 91(5):893–894

Todorovska MI, Trifunac MD (2008) Impulse response analysis of the Van Nuys 7-storey hotel during 11 earthquakes and earthquake damage detection. Struct Control Health Monit: Off J Int Assoc Struct Control Monit Eur Assoc Control Struct 15(1):90–116

Vidal F, Navarro M, Aranda C, Enomoto T (2014) Changes in dynamic characteristics of Lorca RC buildings from pre-and post-earthquake ambient vibration data. Bull Earthq Eng 12:2095–2110

Zerva A, Petropulu AP, Abeyratne U (1996) Blind deconvolution of seismic signals in site response analysis. In: Proceedings of the fifth international conference on seismic zonation (Nice, October 17–19, 1995)

Publisher's Note Springer Nature remains neutral with regard to jurisdictional claims in published maps and institutional affiliations.

Springer Nature or its licensor (e.g. a society or other partner) holds exclusive rights to this article under a publishing agreement with the author(s) or other rightsholder(s); author self-archiving of the accepted manuscript version of this article is solely governed by the terms of such publishing agreement and applicable law.